Random crystal-field effect on magnetic materials

L. Bahmad, A. Benyoussef*, and A. El Kenz

Laboratoire de Magnétisme et Physique des Hautes Energies
Département de Physique, Faculté des Sciences
Avenue Ibn Batouta, B.P 1014 Rabat Morocco

Using the mean field theory, we investigate the effect of the random crystal-field on both the spin-3/2 and spin-2 Blume-Capel models. Several new features are found including the apparence of new ordered phases at low temperature and consequently rich ground state phase diagrams. At finite temperature, new types of phase diagrams are found. Furthermore, we show that at low temperature, first-order transition lines are terminated by isolated critical points, between the ferromagnetic phases.
We also discuss some interesting phenomena such as the existence of compensation and the existence of topologically different types of phase diagrams. The magnetic properties and phase diagrams of this model are presented. The obtained results confirm the existence of new ferri-magnetic phases and consequently the existence of new topologies for the different types of the phase diagrams. Indeed, these phase diagrams present rich varieties of phase transitions with first and second order phase transition lines. These lines are found to be linked by tri-critical points and terminated at isolated critical points. In the case of the spin-2 Blume-Capel model, the interesting finding to emerge consists in the appearance of a new phase, with magnetization (m=3/2), and consequently new types of phase diagrams, divided on topologies depending on the existence of the paramagnetic phase at temperature T=0 K. Finally, the thermal behaviour of the sub-lattices magnetizations, showed the presence of the compensation behaviours for negative values of the crystal-field.

I. INTRODUCTION

The spin-S Blume-Capel model is a generalization of the standard Ising model. It has been originally introduced in the literature by Blume [1] and independently by Capel [2] as an Ising model, with S=1, including single ion anisotropy. Its phase diagram presents a line of continuous transition and a line of first-order transition, separated by a tri-critical point. Later, a generalization of the Blume-Capel model was introduced, the Blume-Emery-Griffiths model [3]: It has been used to study ^{3}He-^{4}He mixtures. In fact, in these mixtures, the state S=0 represents an ^{3}He atom, while ^{4}He atoms are denoted by S=±1 states.
The spin- 1 Blume-Capel system was studied by a variety of methods such as two-spin cluster [4], variational methods [5], constant coupling approximation [6], Monte Carlo simulations [7-9], finite-size-scaling [10-13], renormalization group methods [14-16] and effective field approximation [17-19]. Spin-3/2 models have been introduced earlier to explain phase transition in $DyVO_4$ [20-24] and critical properties in ternary fluid mixtures [25]. Furthermore, different methods have been applied to study the equilibrium properties of these models such as mean field approximation (MFA) [20,25-28], the effective field theory [29-32], renormalization group technique [33-36].

* Member of the Hassan-II Academy of Science and Technology.

On the other hand, the critical behavior of the spin-2 Blume-Capel model is also very interesting to study although this system has not received well deserved attention so far. In fact, for such a high spin value it is really very hard to find and distinguish all the solutions of the model. Experimentally, the spins of Fe^{II} ions or spin-2 and found that these ions have anisotropy [37]. Theoretically, the spin-2 model has been investigated by effective field-theory with correlations [38-40], four-spin model approximation [41], effective field - method within the framework of a single single site cluster theory [42], real space renormalization group [43] and on the Bethe lattice by the use of exact recursion relations [44].
The aim of this work is to investigate, via a MFA, the influence of crystal-field disorder on the magnetic properties of both spin-3/2 and spin-2 Blume-Capel model. However, the effect of a random crystal-field has been studied in different models; spin-1 Ising model [45-48], Blume-Emery-Griffiths model [49], decorated ferrimagnetic Ising model [50] and mixed spin systems [51,52]. In the particular two-valued distribution of crystal-field, given in Ref. [48], a new phase (partly ferromagnetic phase, m=1/2) has been found. Furthermore, this distribution law has been used in the study of decorated [50] and mixed [52] ferrimagnetic systems. Consequently, a most interesting result emerging from these studies is the appearance of new types of phase diagrams. in the case of spin S=2 the partly ferromagnetic phase is given by the magnetization m=3/2 .
In this paper, we introduce and give the details of the MFA for both spin-3/2 and spin-2 Blume-Capel model.

The ground state phase diagrams are discussed for the two models. We also give the phase diagrams and thermal magnetization behaviours for different parameters of the system.

II. MODEL AND FORMULATIONS.

A. Spin-3/2 case.

The Hamiltonian of the spin-3/2 Blume-Capel model is given by:

$$H = -J\sum_{<ij>} S_i S_j + \sum_i \Delta_i S_i^2 \qquad (1)$$

where each S_i located at site i . J (J > 0) is the exchange interaction between nearest-neighbour pairs <ij> and Δ_i is a random crystal-field distributed according to the law:

$$P(\Delta_i) = \frac{1}{2}[\delta(\Delta_i - \Delta(1+\alpha)) + \delta(\Delta_i - \Delta(1-\alpha))] \qquad (2)$$

with $\alpha \geq 0$. To write the mean field equations, let h denotes the molecular field associated with the order parameter m=<S> :

$$h=zJm \qquad (3)$$

where z is a coordination number. The effective Hamiltonian of the system is:

$$H_0 = -h\sum_{i=1}^{N} S_i + \sum_{i=1}^{N} \Delta_i S_i^2 \qquad (4)$$

It generates the following partition function:

$$Z_0=Tr(\exp(-H_0/T))=[2\exp(-9\beta\Delta_i/4)\cosh(3\beta h/2)+2\exp(-\beta\Delta_i/4)\cosh(\beta h/2)+1]^N \qquad (5)$$

We note that the Boltzmann's constant has been set to unity. The variational principle based on the Gibbs-Bogoliubov inequality for the free energy per site is described by :

$$F \leq \Phi=-T\ln(Z_0)+<H-H_0>_0 \qquad (6)$$

and the order parameter m which is the spin average is given by:

$$m=(1/2)(A/B+C/D) \qquad (7)$$

where

$$A=3\sinh(3zm/2t)+\exp(d/t(1+\alpha))\sinh(3zm/2t)$$

$$B=3\cosh(3zm/2t)+\exp(d/t(1+\alpha))\cosh(3zm/2t)$$

$$C=3\sinh(3zm/2t)+\exp(d/t(1-\alpha))\sinh(3zm/2t)$$

$$D=3\cosh(3zm/2t)+\exp(d/t(1-\alpha))\cosh(3zm/2t)$$

In the following, we give a detailed discussion of the ground-state phase diagram. For this purpose we determine the different phases of the system at T=0K for positive values of α. However, Eq.7 has been solved analytically and we have found m=3/2, 1 , and 1/2 . The energies of all possible solutions can easily be calculated. By comparing these energies, the type of the ground state phase diagram, in the (d=Δ/J,α) plane, is then determined as it is seen in Fig. 1. We can distinguish four cases:

i) For $0 \leq \alpha < 1/4$: A first-order transition line between the ferromagnetic $F_{3/2}$ phase (m=3/2) and the ferromagnetic $F_{1/2}$ phase (m=1/2) occurs at (d=z/2). We note that α=1/4 is independent of the coordination number z .

ii) For $1/4 \leq \alpha < 1$, two first-order transition lines between the $F_{3/2}$ phase and the ferromagnetic F_1 phase (m=1) and between the F_1 phase and the ferromagnetic $F_{1/2}$ phase occur at d=5z/(8(1+α)) and d=3z/(8(1-α)) , respectively.

iii) For α =1 , a first order transition line between the $F_{3/2}$ phase and the ferromagnetic F_1 phase occurs at d=5z/16 .

iv) For $\alpha > 1$, two first order transition lines between the F_1 phase, the $F_{3/2}$ phase and the F_1 phase occur at d=5z/(8(1-α)) and d=5z/(8(1+α)) , respectively. We can remark that for large values of α, the region of the phase $F_{3/2}$ become small and the phase F_1 dominates.

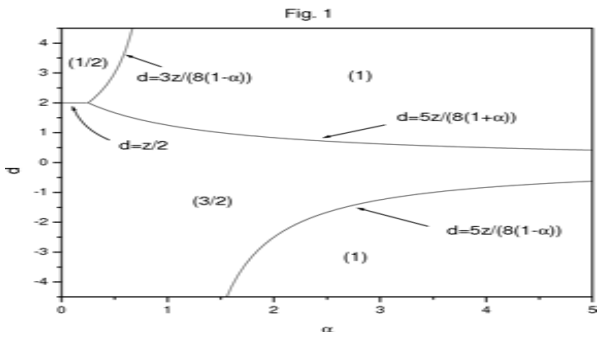

FIG. 1: The ground state phase diagram of the spin-3/2, established in the (d,α) plane. $F_{3/2}$, F_1, $F_{1/2}$ and P represent the ferromagnetic phases m=3/2, 1, 1/2 and the paramagnetic phase m=0, respectively. The coordination number is taken to be z=4 (square lattice).

To discuss the finite temperature phase diagrams, Eq.7 is solved numerically and we choose the solution which minimizes the free energy. However, the phase diagrams in (tc=Tc/J,d) plane, obtained from MFA, are shown in Figs. 2 for selected values of α=0.15 and 0.5. Thus, in Fig. 2a, plotted for α=0.15 , we find the well-known spin-3/2 Blume-Capel's phase diagram in which a second-order transition line separates the ferromagnetic phases ($F_{3/2}$ and F_1) and the paramagnetic phase P (m=0). Moreover, at low

temperature, a first-order transition line between the two ordered phases, which terminates at an isolated critical point (t_{ic}=0.85,d_{ic}=2), appears. Therefore, a continuous passage occurs at temperatures higher than t_{ic}.

This type of phase diagram occurs in the range $0 \leq \alpha < 1/4$. In agreement with the ground-state phase diagram a first-order transition line between the ordered phases $F_{3/2}$ and F_1 is found and follow-up of an other one separating the ordered phases F_1 and $F_{1/2}$ (see Fig. 2b) and terminate at isolated critical points (t_{ic}=0.59,d_{ic}=1.66) and (t_{ic}=0.51,d_{ic}=3), respectively. One can note that the shape of the second-order line separating the ferromagnetic phases and the paramagnetic phase is similar in Figs. 2a and 2b. Indeed, the second-order transition temperature separating the phases P and $F_{3/2}$, which is inserted into the phase F_1, is superior to that one between the phases P and F_1. This is due to a competition between positive and negative values of the crystal-field and therefore the ferromagnetic phase F_1 is favoured with increasing α.

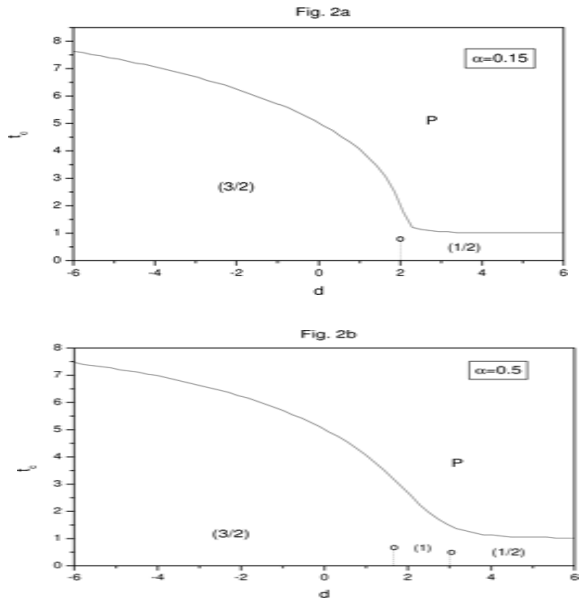

FIG. 2: The critical temperature plotted as a function of d for selected values of α=0.15 (a) and α=0.5 (b). The full and dashed lines represent the second-order and first-order transition lines, respectively. The symbols (o) represent the isolated critical points.

In order to investigate the system behaviour as a function of α we give, in Figs. 3, the reduced transition temperature tc for several values of the reduced crystal-field d. In Fig. 3a, therefore, the temperature tc is depicted for the system with d=-4. As it is seen from this figure, the ordered phases $F_{3/2}$ and F_1 can be located, at low temperature, separated by a first-order transition line which terminate at an isolated critical point. While above them the usual paramagnetic phase become stable, and separated from the ferromagnetic phases by a second-order transition line. The topology of this phase diagram is also analogous to those given for $0 < d < 2$.

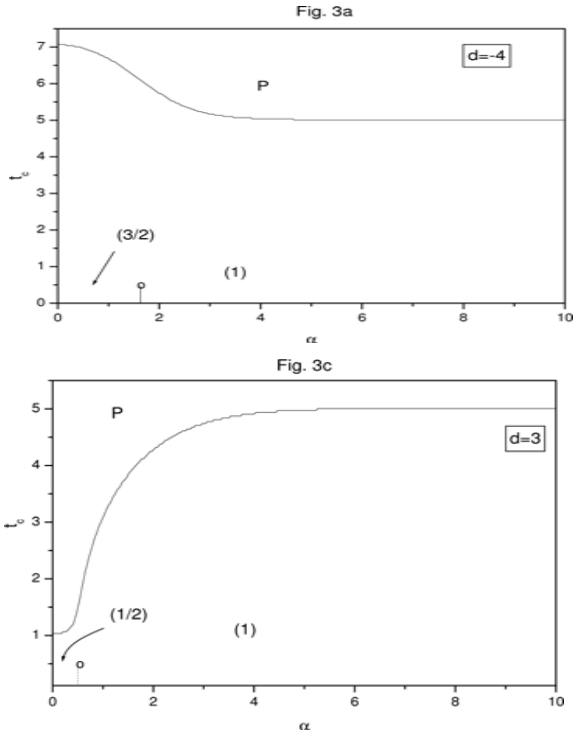

FIG. 3 : The transition temperatures tc as a function of the parameter α for fixed values of the crystal field d: d=-4 (a) and d=3 (b).

Here, one observes the analogous phase diagram as the one given in Fig. 3a but replacing the $F_{3/2}$ by $F_{1/2}$.

As it is seen from Figs. 3a and Fig. 3b, the shape of the second-order transition line between the ferromagnetic phases and the paramagnetic phase depends on the value of spin in each order phase. Indeed, the second-order transition temperature increases with the values of spins (m=3/2 , 1, 1/2) .

It is known that the role of the crystal-field is important for magnetizations of the Ising systems. The temperature and crystal dependence of magnetizations in the spin- 3/2 Blume-Capel model are calculated by solving Eq.7 numerically. We restrict ourselves to investigate the behaviour of the magnetization in the two case α=0.5. The thermal variation of the magnetization is plotted for selected values of d=1, 2.5 and 5 (see Fig. 4a). Thus the magnetization m starts at 3/2, 1 and 1/2 for d=1, 2.5 and 5 , respectively, and vanishes continuously at second-order transition temperature. In Fig. 4b, the reduced crystal-field dependence on magnetization is depicted for t=0.25 ad t=1.

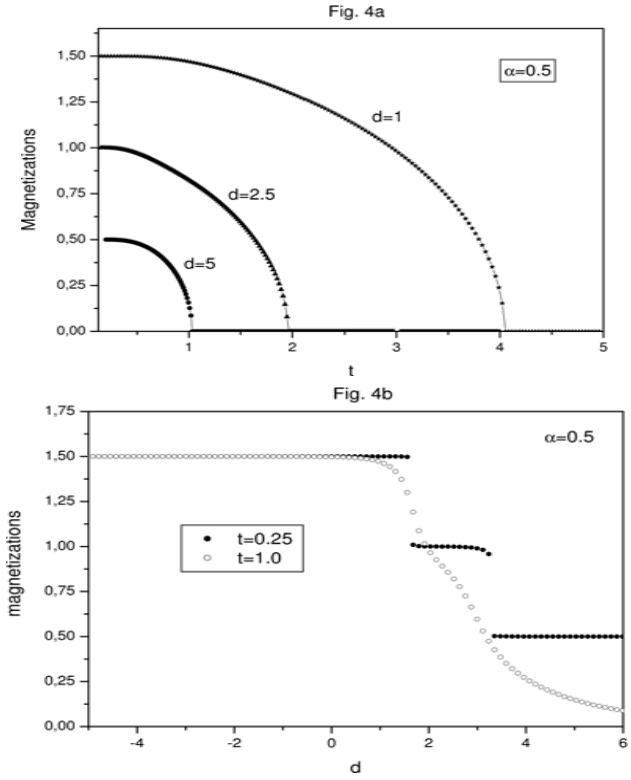

FIG. 4: The magnetization behavior as a function of the temperature (a), and reduced crystal-field (b) for α= 0.5. In Fig. (a), d is taken to be d=-1, 2.5 and 5. Whereas, the magnetization is plotted in (b), for two temperatures below and above the isolated critical points: t=0.2 and t=1, respectively. Magnetic plateaus and continuum passage are seen in this figure.

For a temperature lower than the value corresponding to the isolated critical point t_{ic}, t=0.25 , a successively first-order transition between the phases $F_{3/2}$ and F_1 at d=1.67 and between the phases F_1 and $F_{1/2}$ at d=3.35 . Whereas, a continuous passage occurs between these phases for t=1 , which is higher than t_{ic}. In the second case, for t=5.5 a reentrant phenomenon is observed for negative values of crystal-field d.

B. Spin-2 case.

The Hamiltonian of the spin-2 Blume-Capel model is given by Eq. (1). where each S_i located at site i is a spin-2 with five discrete spin values: 0, ±2 and ±1. The random crystal-field Δ_i is distributed according to the law (2). To write the mean field equations, let h denotes the molecular field associated with the order parameter m=<S> : $h=zJm$ where z is a coordination number taken to be 4 (square lattice). The effective Hamiltonian of the system is:

$$H_0 = -h\sum_{i=1}^{N} S_i + \sum_{i=1}^{N} \Delta_i S_i^2 \qquad (8)$$

It generates the following partition function:

$$Z_0=Tr(\exp(-H_0/T)) =[2\exp(-4\beta\Delta_i)\cosh(2\beta h)+2\exp(-\beta\Delta_i)\cosh(\beta h)+1]^N \qquad (9)$$

the Boltzmann's constant has been set to unity.
The variational principle based on the Gibbs-Bogoliubov inequality for the free energy per site is described by Eq. *(7)* and the order parameter which is the spin average is given by:

$$m=(1/2)(N1/D1+N2/D2) \qquad (10)$$

where

$$N1=4\exp(-4d/t(1+\alpha))\sinh(2zm/T)+2\exp(-d/t(1+\alpha))\sinh(2zm/T)$$

$$D1=2\exp(-4d/t(1-\alpha))\sinh(2zm/T)+2\exp(-d/t(1+\alpha))\cosh(zm/T)+1$$

$$N2=4\exp(-4d/t(1-\alpha))\sinh(2zm/T)+2\exp(-d/t(1-\alpha))\sinh(2zm/T)$$

$$D2=2\exp(-4d/t(1-\alpha))\sinh(2zm/T)+2\exp(-d/t(1-\alpha))\cosh(zm/T)+1$$

The total free energy can be written as:

$$f=(-t/2)[\ln[2\exp(-4d/t(1+\alpha))\cosh(2zm/T)+2\exp(-d/t(1+\alpha))\cosh(zm/t)+1]+\ln[2\exp(-4d/t(1-\alpha))\cosh(2zm/t)+2\exp(-d/t(1-\alpha))\cosh(zm/t)+1] \qquad (11)$$

Usually, the solutions of the Eq. (10) will not be unique, the stable ones are those minimizing the free energy (Eq.11), while the others are the unstable ones. If the order parameter is continuous (discontinuous), the transition is of second (first) order.
Before obtaining and discussing the phase diagrams, first we have to study analytically the ground state phase diagram to determine different phases of the system. In fact, for T=0K and $\alpha \geq 0$, Eq. (10) has five solutions: m=2, 3/2, 1, 1/2 and 0. The energies of all possible solutions can easily be calculated. By comparing these energies, the type of the ground state phase diagram, in the ($d=\Delta/J,\alpha$) plane, is then determined as it is seen in Fig. 5. We can distinguish several cases in different topologies of phase diagrams depending on the appearance of the paramagnetic phase P (m=0) at T=0K or not.

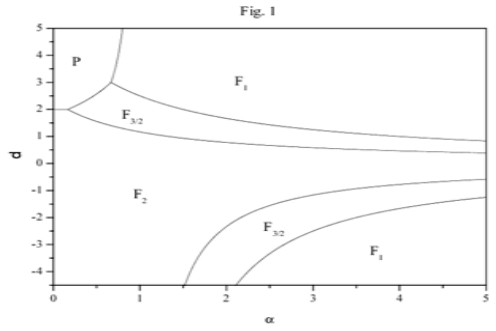

FIG. 5: The ground state phase diagram of the spin-2, established in the (d,α) plane. F_1, $F_{3/2}$, F_2 and P represent the ferromagnetic phases (m=1, 3/2, 2) and the paramagnetic phase (m=0), respectively.

i) For $0 \le \alpha \le 1/6$: A first-order transition line between the ferromagnetic F_2 (m=2) and the paramagnetic one occurs at (d=z/2).

ii) For $1/6 < \alpha \le 2/3$: Successive first-order transition lines between the phase F_2 and the new ferromagnetic phase $F_{3/2}$ (m=3/2 at $d=7z/(12(1+\alpha))$ and between the last phase and the phase P at $d=9z/(4(5-3\alpha))$. Furthermore, $\alpha=1/6$ and $\alpha=2/3$ are independent of coordination number z .

iii) For $2/3 < \alpha < 1$: In addition to the phase transition between F_2 and $F_{3/2}$ an other first-order transition line between the phases $F_{3/2}$ and F_2 occurs at $d=5z/(4(1+\alpha))$, and followed by a first-order transition between the phases F_1 (m=1) and P at $d=z/(4(1-\alpha))$.

iv) For $\alpha=1$: It is the first case in the second topology of the phase diagrams in which the paramagnetic phase disappear at T=0K and consequently the transition between the phases F_1 and P, in the above paragraphs, dos not occur.

v) For $\alpha > 1$: In this case the ferromagnetic phases $F_{3/2}$ and F_1, which appears for positive values of the crystal-field can also occur for $d < 0$. Thus, in addition to the transitions cited in the case iv), first-order transitions between the phases $F_{3/2}$ and F_2 and the phases F_1 and $F_{3/2}$ occur at $d=7z/(12(1-\alpha))$ and $d=5z/(4(1-\alpha))$, respectively. In fact, they give rise to two different phase diagrams.

Now, let us turn to a detailed discussion dealing with the finite temperature phase diagrams. For this purpose, Eqs.10 and 11 are solved numerically and we choose the solution that minimize the free energy. However, the phase diagrams in (tc=Tc/J,d) plane, obtained from MFA, are shown in Figs. 6 for selected values of α=0.1 and 0.5. Thus, in Fig. 6a, plotted for α=0.1 , we find a phase diagram which is analogous to that one of the spin-1 Blume-Capel model. Indeed, second-order transition and first-order transition lines which are linked by a tri-critical temperature located at (t_{tr}=1.65,d_{tr}=1.98). These transition lines separate the ferromagnetic phase F_2 and the paramagnetic phase P . This type of phase diagram occurs in the range $0 \le \alpha$

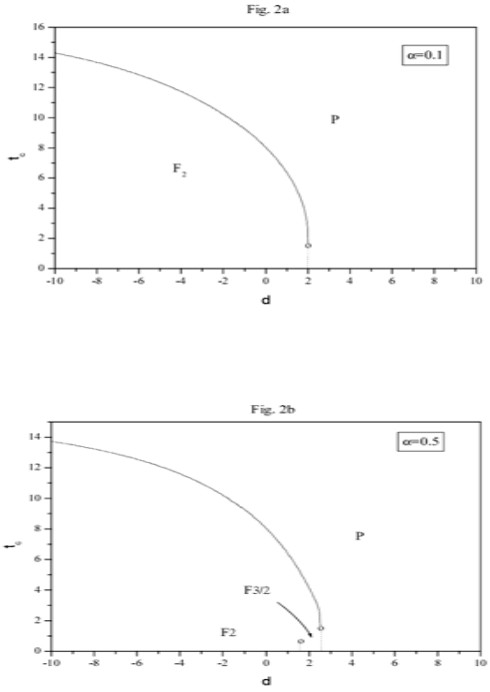

FIG. 6: The critical temperature plotted as a function of the crystal-field for selected values of α =0.1 (a), α =0.5 (b), The full and dashed lines represent the second-order and first-order transition lines, respectively. The black and white circles denote the tri-critical and isolated critical points, respectively.

However, this phenomenon has been observed in Fe^{++} which has spi-0 and spin-2 for large and low crystal-field, respectively.

For $1/6 \le \alpha < 2/3$ the ferromagnetic $F_{3/2}$ appears, at low temperature, and it is separated from the phase F_2 by a first-order transition line which terminates at an isolated critical point (t_{ic}=0.60, d_{ic}=1.55) as it is shown in Fig. 6b.

However, as it is known, the critical temperature between the ferromagnetic phase and the paramagnetic one increases with the value of spin. We should mention that, for large values of α, the region of the ferromagnetic phase F_1 dominates as it is shown in the ground state phase diagram.

In order to discuss the effect of α on the phase diagrams,we have plotted in Figs. 7 the behaviors of

critical temperature tc depending on α for selected values of d. Thus, in Fig. 7a, plotted for d=-3, two first-order transition lines appear and separate the phase F_2 from the phase $F_{3/2}$ and the phase $F_{3/2}$ from the phase F_1 and terminate at isolated critical points (t_{ic}=0.48, α_{ic}=1.78) and (t_{ic}=0.45, α_{ic}=2.67), respectively. This behavior of phase diagram is similar to that one given at low temperature. On the other hand, at high temperature, the second-order transition temperature between the ferromagnetic phases and the paramagnetic phase decreases with increasing α in Fig. 7a .

In Fig. 7b the paramagnetic phase appears at T=0K. In fact, the second-order transition line between the ordered phases and the disordered phase, is linked, by a tri-critical point (t=1.55,α=0.47), with the first-order transition line which flows to a zero temperature. We note that the phase $F_{3/2}$ and consequently we have a phase transition between F_1 and P phases.

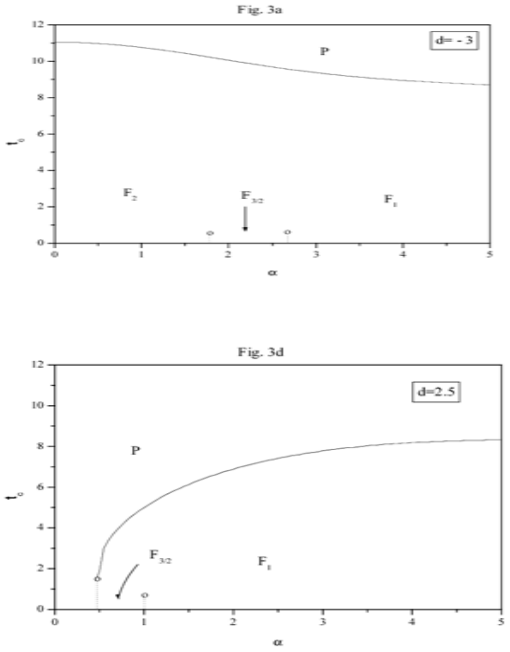

FIG. 7: The transition temperatures t_c as a function of the parameter α for fixed values of the crystal field d: d=-3 (a), and d=2.5 (b) .

It is known that the role of the crystal-field is important for magnetization of the Ising systems. The temperature and crystal-field dependence of magnetization are calculated by solving Eqs. (10) numerically. Indeed, in Fig. 8a, the dependence of magnetization on temperature is depicted for selected values of d=-1, 0, 2 and 3.5 . The magnetization m starts at 2, 3/2 and 1 for d=-1 0, 2 and 3.5 , respectively. Furthermore, m decreases continuously and vanishes at second-order transition temperature. Furthermore, the magnetization m decreases continuously and vanishes at second-order transition temperature. At low temperature. In fact, we give this magnetization dependence of d in Fig 7b. It is seen that four magnetization plateaus appear, located at m=2, 3/2, 1 and 0, which is in good agreement with the ground state phase diagram. The appearance of these magnetic plateaus has been found in the one-dimensional antiferromagnetic spin-2 Ising chains with single-ion anisotropy in the presence of an external magnetic field at very low temperature. Above the isolated critical points, continuous passage between the ferromagnetic phases F_2, $F_{3/2}$ and F_1 and a first-order temperature between these phases and the paramagnetic phase P occur.

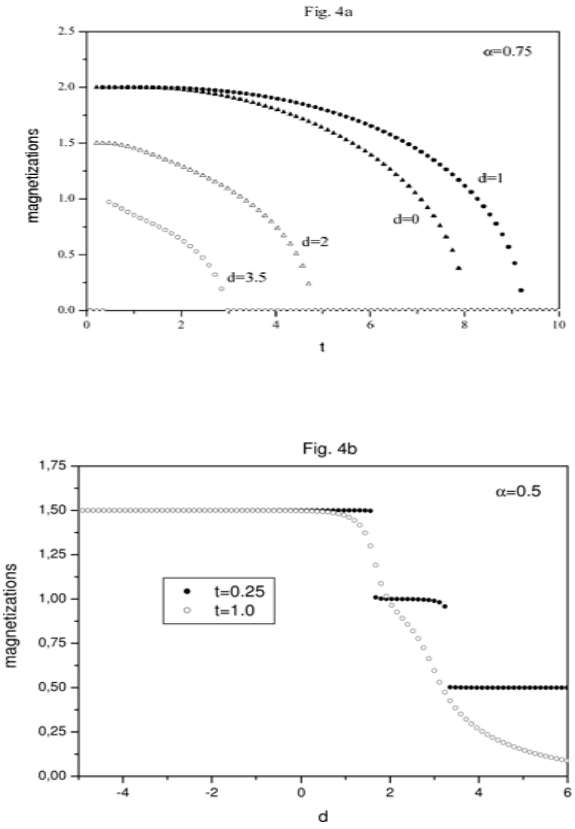

FIG. 8: The behavior of the magnetization as a function of the temperature in (a), for α=0.75 and d=-1, 0, 2 and 3.5. and in (b), for α=3 and d=-4, -2.1, 0, 0.9 and 3.5. Magnetic plateaus and continuum passage can be seen in these figures.

III.CONCLUSION

We have studied the effect of a random crystal-field on both spin-3/2 and spin-2 Blume-Capel model using the mean field approximation. In fact, an interesting finding consists in the appearance of a new phase in the spin-3/2 case, with magnetization m=1, and consequently a rich variety of phase diagrams. Indeed, at low temperature and depending on the values of α, first-order transition lines terminated at isolated critical points, between the ferromagnetic phases: 3/2, 1 and 1/2 appear. Whereas, at higher temperature, a second-

order transition line between the ordered phases and the disordered phase occurs.

In the the spin-2 Blume-Capel model case, we showed the existence of a new phase, with magnetization m=3/2 , and consequently the appearance of new types of phase diagrams. In fact, these phase diagrams were divided on two topologies depending on the existence of the paramagnetic phase or not at T=0 K. At low temperature, and depending on the values of α, we found a succession of first-order transition lines between the ferromagnetic phases F_2, $F_{3/2}$ and F_1 which terminate at isolated critical points. Whereas, at high temperature, a second-order transition line between the ferromagnetic phases and the paramagnetic phase occurs.

References

[1] H. W. Capel, Physica **32**, 966 (1966).
[2] M. Blume, Phys. Rev. **141,** 517 (1966).
[3] M. Blume, V. J. Emery and R. B. Griffiths, Phys. Rev. **A 4,** 1071 (1971).
[4] S. L. Lock and B. S. Lee, Phys. Stat. Sol. **B 124,** 593 (1984).
[5] W. Man Ng and J. H. Barry, Phys. Rev. **B 17,** 3675 (1978).
[6] M. Tanaka and K. Takahashi, Phys. Stat. Sol. **B 93,** K85 (1979).
[7] A. K. Jain and D. P. Landau, Phys. Rev. **B 22,** 445 (1980).
[8] O. F. de Alcantara Bonfim and C. H. Obcemea, Z. Phys. **B 64**, 469 (1986).
[9] N. B. Wilding and P. Nielaba, Phys. Rev. **E 53**, 926 (1996).
[10] P. D. Beale, Phys. Rev. **B 33**, 1717 (1986).
[11] F. C. Alcaras, J. R. D. de Felicio, R. Koberle and J. F. Stilck, Phys. Rev. **B 32**, 7969 (1985).
[12] D. B. Balbao and J. R. D. de Felicio, J. Phys. A: Math. Gen. **20**, L207 (1987).
[13] J. V. Gehlen, J. Phys. A: Math. Gen. **24**, 5371 (1990).
[14] A. N. Berker and M. Wortis, Phys. Rev. **B 14**, 4946 (1986).
[15] O. F. de Alcantara Bonfim, Physica **A 130**, 367 (1985).
[16] S. M. de Oliveira, P. M. C. de Olivera and F. C. de Sa Barreto, J. Stat. Phys. **78**, 1619 (1995).
[17] X. F. Jiang, J. L. Li and J. L. Zhong, Phys. Rev. **B 47**, 827 (1993).
[18] K. G. Chakraborty, Phys. Rev. **B 29**, 1454 (1984).
[19] A. F. Siqueria and I. P. Fittipaldi, Phys. Rev. **B 31**, 6092 (1985).
[20] J. Sivardiere, M. Blume, Phys. Rev. **B 5**, 1126 (1972).
[21] A. H. Cooke, D. M. Martin, M. R. Wells, J. Phys. (Paris). Colloq. **32**, C1 (1971).
[22] A. H. Cooke, C. J. Ellis, K. A. Gehring, M. I. M. Leask, D. M. Martin, B. M. Wanklyn, M. R. Wells and R. L. White, Solid State Commun. **8**, 689 (1970).
[23] A. H. Cooke, D. M. Martin, M. R. Wells, Solid State Commun. **9**, 519 (1971).
[24] F. Sayetat, J. X. Boucherbe, M. Belakhovsky, A. Kallal, F. Tcheou and H. Fuess, Phys. Lett. **34 A**, 361 (1971).
[25] S. Krinsky and D. Mukamel, Phys. Rev. **B 11**, 399 (1975).
[26] F. C. Sa Barreto, O. F. de Alcantara Bonfimn, Physica **A 172**, 378 (1991).
[27] A. Bakchich, S. Bekhechi and A. Benyoussef, Physica A **210**, 415 (1994).
[28] O. Ozsoy and M. Keskin, Physica **A 319**, 404 (2003).
[29] T. Kaneyoshi and M. Jascur, Phys. Lett. **A 177**, 172 (1993).
[30] L. Peliti and M. Saber, Phys. Stat. Sol. **B 195**, 537 (1996).
[31] W. Jiang, G. Z. Wei, Z. H. Xin, Phys. Stat. Sol. **B 219**, 157 (2000).
[32] Y. Q. Liang, G. Z. Wei, Q. Zhang and Z. H. Xin, J. Magn. Magn. Mater. **267**, 275 (2003).
[33] A. Bakchich, A. Bassir and A. Benyoussef, Physica **A 195**, 118 (1993).
[34] N. Tsushima, Y. Honda and T. Horuguchi, J. Phys. Soc. Jpn. **66**, 3053 (1997).
[35] N. Tsushima and T. Horuguchi, J. Phys. Soc. Jpn. **67**, 1574 (1998).
[36] W. J. Song and C. Z. Yang, Solid State Commun. **91,** 145 (1994).
[37] C. Mathoniere, C. J. Nutall, S. G. Carling, P. Day, Inorg. Chem. 35 1201 (1996).
[38] W. Jiang, G. Z. Wei, Z. H. Xin, Phys. Stat. Sol. (b) 221 759 (2000).
[39] Y. Q. Liang, G. Z. Wei, Q. Zhang, Chinese Phys. Lett. 21 378 (2004).
[40] Y. Q. Liang, G. Z. Wei, L. L. Song, G. L. Song, S. L. Zhang, Commun. Theo. Phys. 42 623 (2004).
[41] T. Iwashita, R. Satou, T. Imada, T. Idogaki, Physica B 284 1203 (2000).
[42] M. Saber, J. W. Tucker, Physica A 217 407 (1996).
[43] F. C. Sa Barreto, Revista Brazileira de fisica 20 152 (1990).
[44] A. Erdinc, O. Canko and E. Albayrak, Eur. Phys. J. B 52 521 (2006).
[45] A. Benyoussef, T. Biaz, M. Saber and M. Touzani, J. Phys. C: Solid State Phys. 20 5349 (1987).
[46] N. S. Branco, B. M. Boechat, Rev. B 56 11673 (1997).
[47] T. Kaneyoshi, J. Phys. C: Solid State Phys. 21 L469 (1988).
[48] N. Boccara, A. El Kenz, M. Saber, J. Phys: Condens. Matter 1 5721 (1989).
[49] V. Urumov, J. Phys: Condens. Matter 1 7037 (1989).
[50] A. Benyoussef, A. El Kenz, M. El Yadari, to appear in Physica B (2007)
[51] T. Kaneyoshi, Physica A 153 556 (1988).
[52] L. Bahmad, A. Benyoussef and A. El Kenz submitted to Physica A.